Modeling of Pyrolysis and Opposed Flow Flame Spread Over Charring Materials

Arvind Atreya

Department of Mechanical Engineering

University of Michigan, Ann Arbor, MI 48109

and

Howard R. Baum

Building and Fire Research Laboratory, NIST

Gaithersburg, MD 20899

Acknowledgements

Objectives

For large-scale fire models, we need a somewhat simpler description of the solid-phase behavior.

Broadly speaking, burning objects in a fire may be categorized into:

- Those that may be approximated as "vaporizing" at the surface (like PMMA) – an adequate treatment (at least for now), and

- Those that char on the surface (like wood).

While the actual decomposition process for both type of materials is quite complex, the question is:

What is the simplest treatment that captures the essential flame spread physics for charring materials and what are the differences caused by charring?

Outline of the Presentation

- A discussion of the use of pyrolysis temperature models for describing charring materials.

  - How to determine an appropriate pyrolysis temperature for predicting the fuel evolution rate from charring materials?

  - Is it a material property?

  - How accurate is such a treatment?

- A model of flame spread over charring materials using the pyrolysis temperature concept.

- Discussion of the model – the effect of charring.

- Conclusions.

Pyrolysis Temperature Assumption

We first examine the pyrolysis temperature assumption by considering two otherwise identical models:

- one with finite rate decomposition kinetics, and

- the other with infinite rate kinetics (pyrolysis temperature)
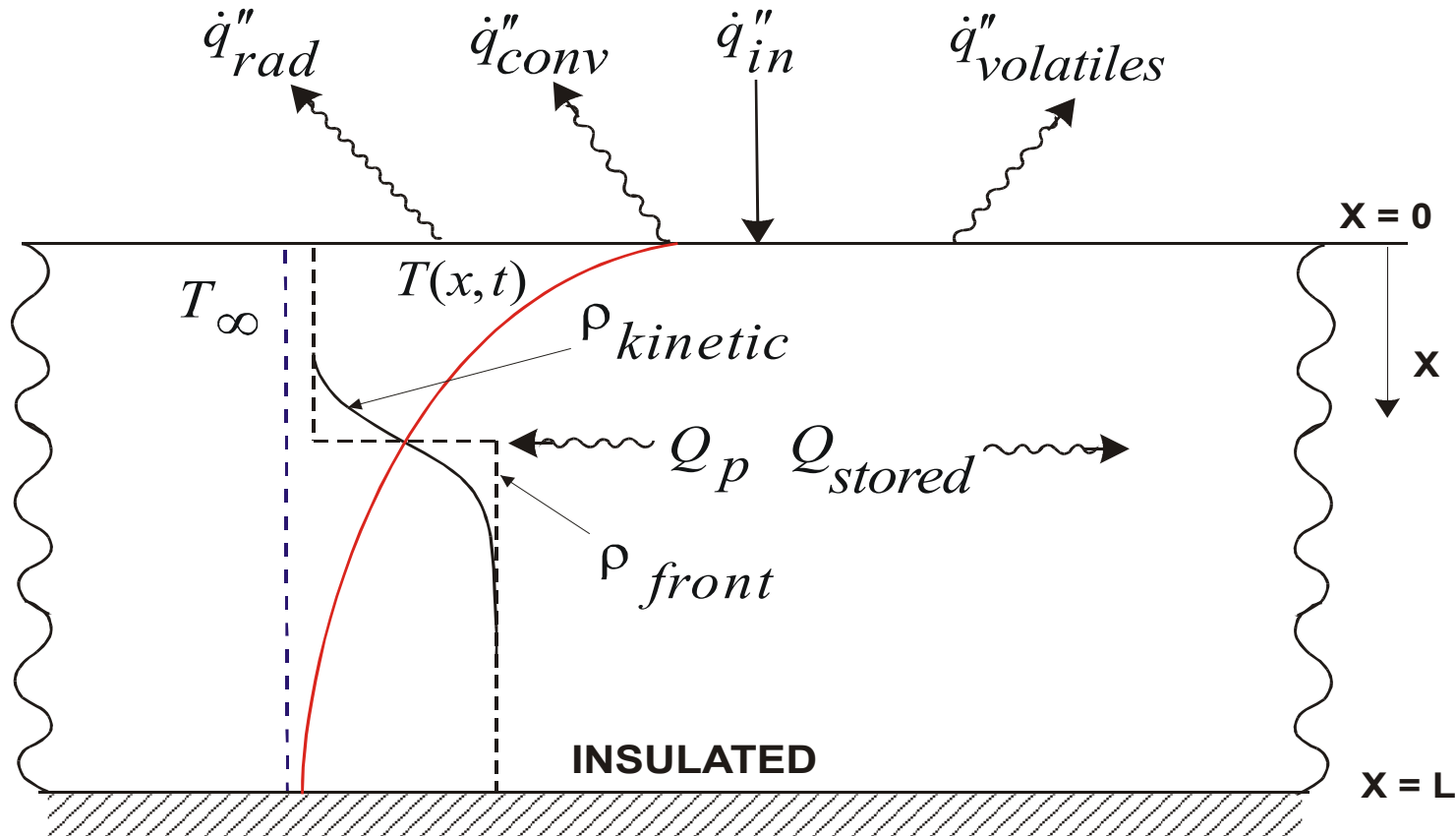
Physical configuration of the problem considered.

Energy equation : $\dfrac{\partial}{\partial t}\left(\rho_s h_s\right) = \dfrac{\partial}{\partial x}\left(k_s \dfrac{\partial T}{\partial x}\right) + Q$, where :

$$Q = Q_p\left(\dfrac{\partial \rho_s}{\partial t}\right) = -AQ_p(\rho_s - \rho_f)\exp(-E/RT)\,;\text{for finite rate kinetics}$$

$$Q = -Q_p(\rho_w - \rho_f)\dfrac{dx}{dt}\,\delta(x - x_p)\,;\text{ for infinite rate kinetics}$$

Initial condition:

$$T(x, 0) = T_\infty\,;\ \rho_c(x, 0) = 0\,;\ \rho_s(x, 0) = \rho_w = \rho_a(x, 0)$$

Boundary conditions:

$$-k_s\dfrac{\partial T}{\partial x}\bigg|_{x=0} = \dot{q}''_{in} - h\big[T(0, t) - T_\infty\big] - \varepsilon\sigma\big[T^4(0, t) - T^4_\infty\big]$$

$$-k\dfrac{\partial T}{\partial x}\bigg|_{x=L} = 0$$

Overall Energy and Mass Balance

If t_f is the time to completely pyrolyze a slab of wood of thickness, L. Then, the total mass of volatile gases produced during the time t_f and the sum of all energies lost, stored and absorbed during the pyrolysis process must be the same as the total input energy and also the same for both the models.

Mass balance: For constant initial (ρ_w) and final (ρ_f) densities, the total mass evolved per unit area $[(\rho_w - \rho_f)L]$ is automatically balanced for both models.

Energy balance:

$$E_{in} = \dot{q}''_{in}\, t_f = \underbrace{\rho_f C_{pc} \int_0^L \left[T(x, t_f) - T_\infty \right] dx}_{E_{st}} + \underbrace{Q_p\,(\rho_w - \rho_f) \cdot L}_{E_{py}}$$

$$+ \underbrace{\int_0^{t_f} \left(\varepsilon\sigma\,(T_s^4(t) - T_\infty^4) + h\,(T_s - T_\infty) \right) dt}_{E_{loss}} + \text{carried out by pyrolysis products.}$$

Energy carried out by the products of pyrolysis is:

for finite rate kinetics

$$= -\int_0^{t_f} \int_0^L \left(\frac{\partial \rho_s}{\partial t} \; \frac{(\rho_w C_{pw} + \rho_f C_{pc})}{(\rho_w - \rho_f)} \; (T(x,t) - T_\infty) \right) dx \, dt$$

for pyrolysis temperature

$$= (\rho_w C_{pw} + \rho_f C_{pc}) (T_p - T_\infty) L.$$

This is the primary difference. Equating the two gives us the energy and mass balanced pyrolysis temperature as:

$$\theta_p = A^* \int_0^1 \int_0^1 \rho_s^* \, \theta \, \exp(-\phi/(\theta+1)) \, d\xi \, d\tau \qquad \text{need} \quad \begin{array}{c} \rho_s^*(x,t) \\ \theta(x,t) \end{array} \; \&$$

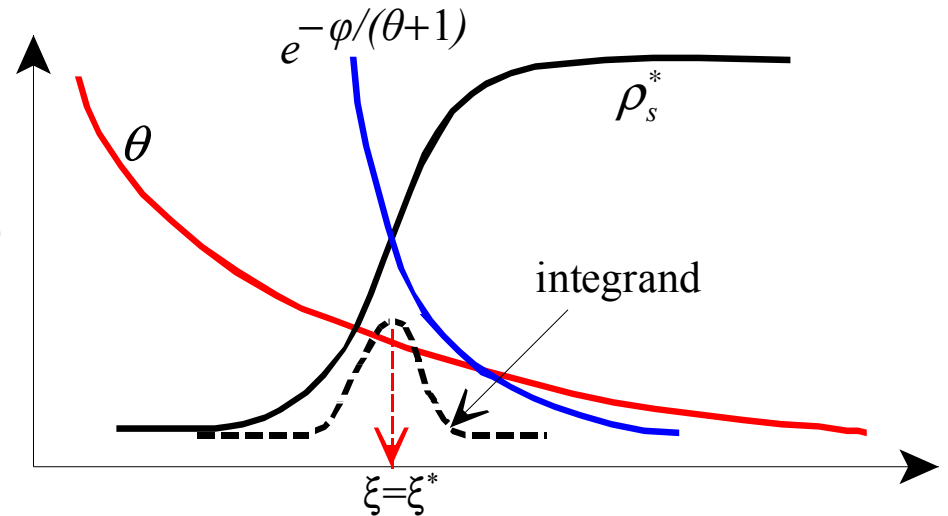Where: $\theta(x,t) = (T(x,t) - T_\infty)/T_\infty \; ; \; \xi = x/L \; ; \; \tau = t/t_f$

$$\rho_s^* = (\rho_s(x,t) - \rho_f)/(\rho_w - \rho_f) \; ; \; \phi = E/RT_\infty \; \& \; A^* = A t_f$$

Estimate by steepest descent. the maximum occurs when:

$$g(\xi^*, \tau) = -\varphi/(\theta+1) + \ln(\rho_s^* \theta)$$

is a maximum, i.e. $g(\xi^*, \tau) = 0$

For large $\left| g_{\xi\xi}(\xi^*, \tau) \right|$
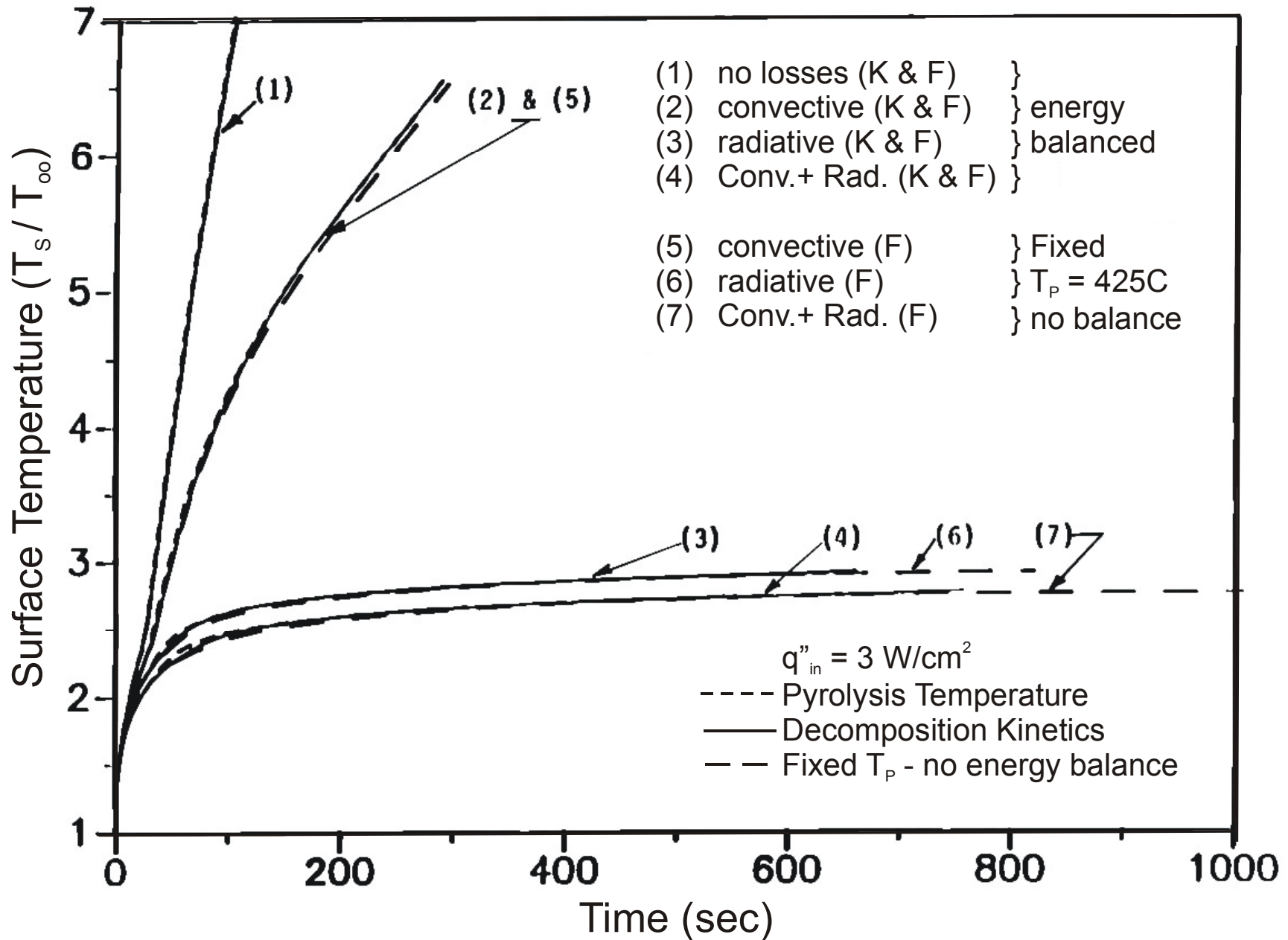

It can be shown that:

$$\theta_p \approx \frac{A^*\sqrt{2\pi}}{e} \; \frac{\theta^* \; e^{-\varphi/(\theta^*+1)}}{\phi/(\theta^*+1)^2} \int_0^1 \frac{d\tau}{\left| \theta_{,\xi}(\xi^*,\tau) \right|}$$
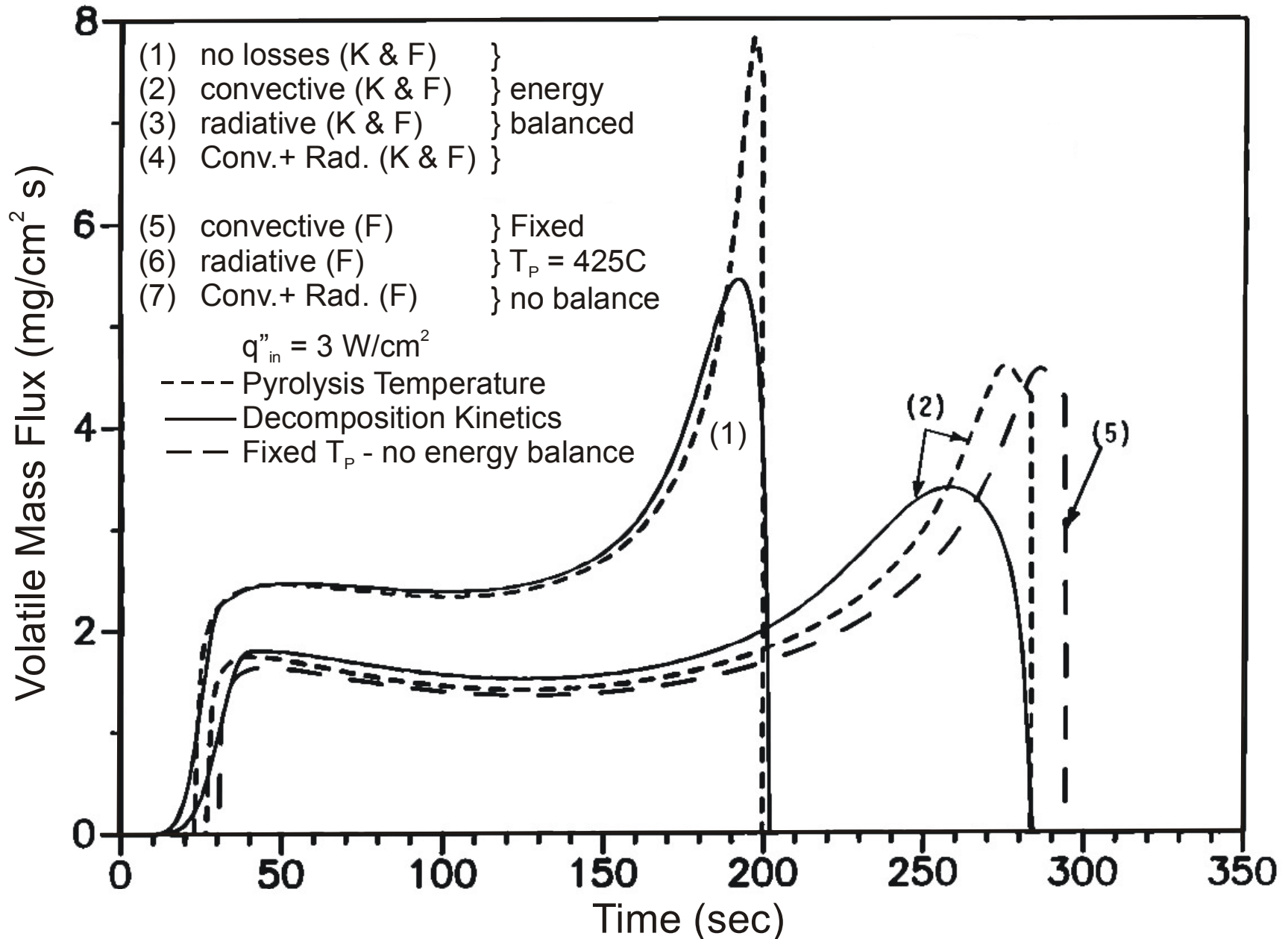
Stuck!! But an approximate formula of energy & mass balanced pyrolysis temperature is attractive because it relates the pyrolysis temperature to kinetic parameters.

Re-start numerically:

Surface temperature for kinetic & pyrolysis temperature models

Surface Temperature (T_S / T_{oo}) vs Time (sec)

(1) no losses (K & F)   }
(2) convective (K & F)   } energy
(3) radiative (K & F)   } balanced
(4) Conv.+ Rad. (K & F) }

(5) convective (F)   } Fixed
(6) radiative (F)   } T_P = 425C
(7) Conv.+ Rad. (F)   } no balance

$q"_{in}$ = 3 W/cm^2
---- Pyrolysis Temperature
—— Decomposition Kinetics
— — Fixed T_P - no energy balance

Volatile mass flux for kinetic & pyrolysis temperature models

Legend within figure:

(1) no losses (K & F)   }
(2) convective (K & F)   } energy
(3) radiative (K & F)   } balanced
(4) Conv.+ Rad. (K & F)   }

(5) convective (F)   } Fixed
(6) radiative (F)   } $T_P = 425C$
(7) Conv.+ Rad. (F)   } no balance

$q"_{in} = 3\ W/cm^2$
- - - - Pyrolysis Temperature
——— Decomposition Kinetics
— — Fixed T_P - no energy balance

Y-axis: Volatile Mass Flux ($mg/cm^2\ s$)
X-axis: Time (sec)

Volatile mass flux for kinetic & pyrolysis temperature models

(5) convective (F)
(6) radiative (F)
(7) Conv.+ Rad. (F)

(1) no losses (K & F)
(2) convective (K & F)
(3) radiative (K & F)
(4) Conv.+ Rad. (K & F)

(4)
(3)
(6)
(7)

q''_{in} = 3 W/cm^2
- - - - Pyrolysis Temperature
——— Decomposition Kinetics
— — Fixed T_P - no energy balance

Volatile Mass Flux (mg/cm^{2}s)

1.2
0.8
0.4
0.0

0   200   400   600   800   1000
Time (sec)

Constants used for the calculations

$$A = 250 \times 10^6 \; 1/\sec \; ;$$

$$C_p = 712 \; J/Kg\,K \; ;$$

$$C_{pw} = 1465.1 \; J/Kg\,K \; ;$$

$$E = 125.58 \times 10^6 \; J/Kg\,mole$$

$$K_c = 0.0712 \; W/m\,K \; ;$$

$$K_w = 0.1675 \; W/m\,K \; ;$$

$$h = 11.4 \; W/cm^2 K \; ;$$

$$Q_p = 30 \; cal/gm$$

$$T_\infty = 25 \; °C \; ;$$

$$\varepsilon = 0.95 \; (surface\ emissivity)$$

$$\sigma = 5.67 \; x \; 10^8 \; W/cm^2 K^4 \; ;$$

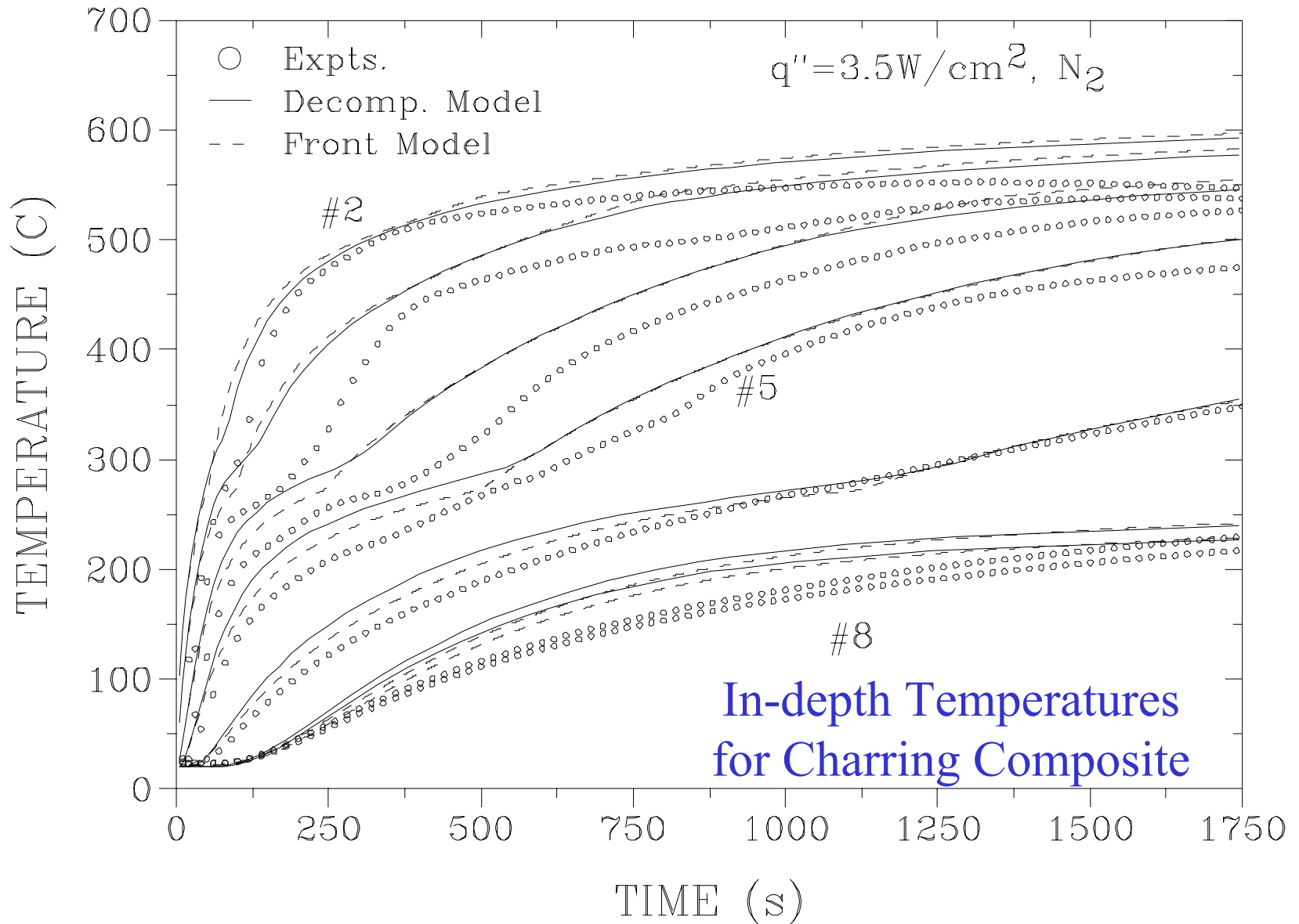$$\rho_w = 676 \; Kg/m^3$$

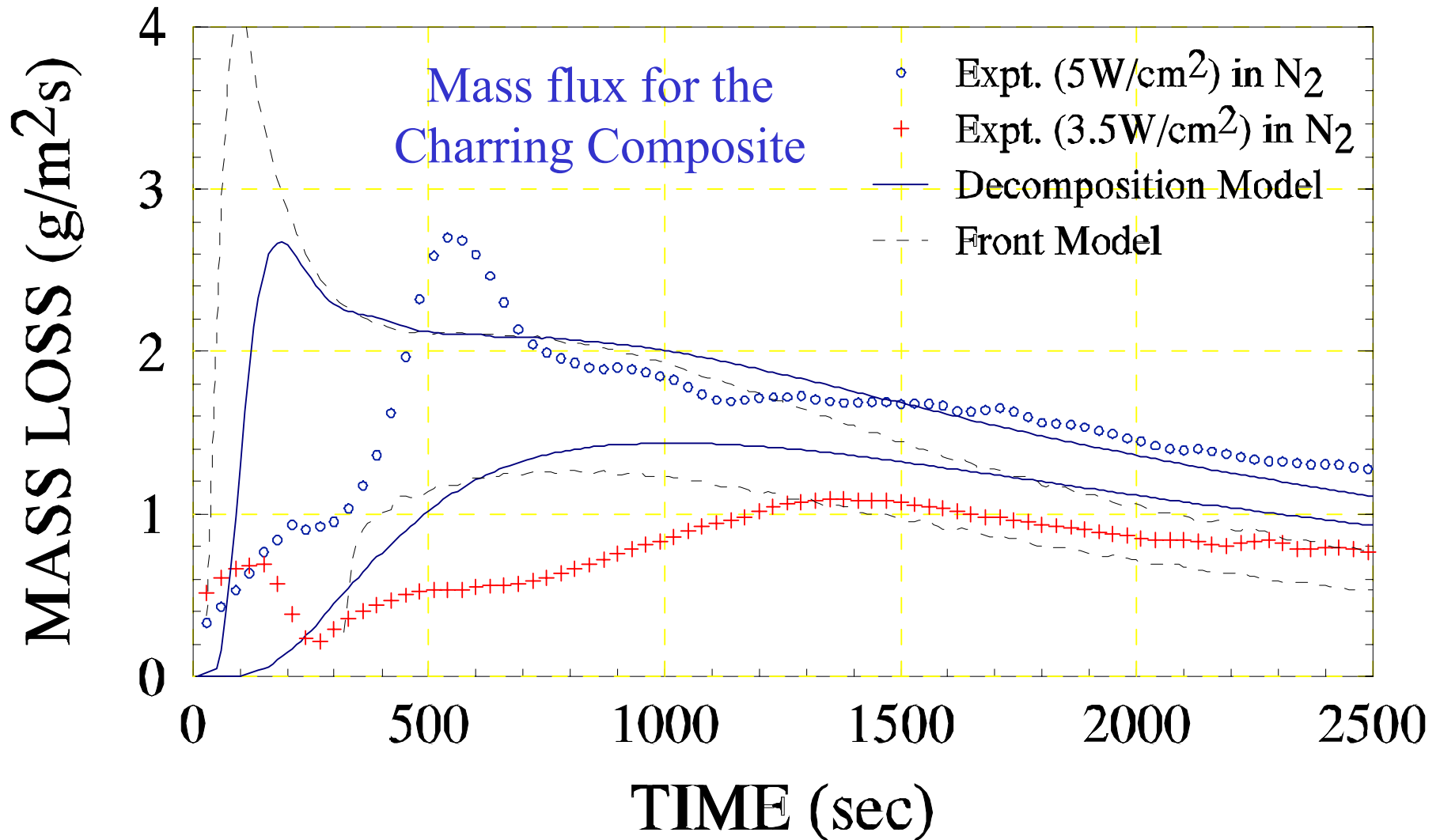$$\rho_c = 162.24 \; Kg/m^3 \; ;$$

$$L = 1 \; cm$$

Percentage difference between the total input energies (E_{in}) for the two models

	Total input energy (Joules)			Percentage difference	
	KINETIC (1)	FRONT (2)	FRONT (3)	(1) & (2)	(1) & (3)
1) no surface heat losses	6.100E+6	5.985E+6 (Tp=425 C)	5.985E+6 (Tp=425°C)	1.87	1.87
2) convective heat losses	8.640E+6	8. 500E+6 (Tp=405 C)	8.820E+6 (Tp=425°C)	1.62	2.08
3) radiative heat losses	19.80E+6	20.00E+6 (Tp=375 C)	24. 600E+6 (Tp=425°C)	1.01	24.24
4) convective and radiative heat losses	22.679E+6	21.11E+6 (Tp=350 C)	30.200E+6 (Tp=425°C)	6.90	33.05

Comparison of Arrhenius & Front Models with Experiments

Expts.
Decomp. Model
Front Model

$q''=3.5W/cm^2$, N_2

#2

#5

#8

In-depth Temperatures
for Charring Composite

TEMPERATURE (C)

TIME (s)

Comparison of Arrhenius & Front Models with Experiments

Mass flux for the Charring Composite

Legend:
- Expt. ($5W/cm^2$) in N_2
- Expt. ($3.5W/cm^2$) in N_2
- Decomposition Model
- Front Model
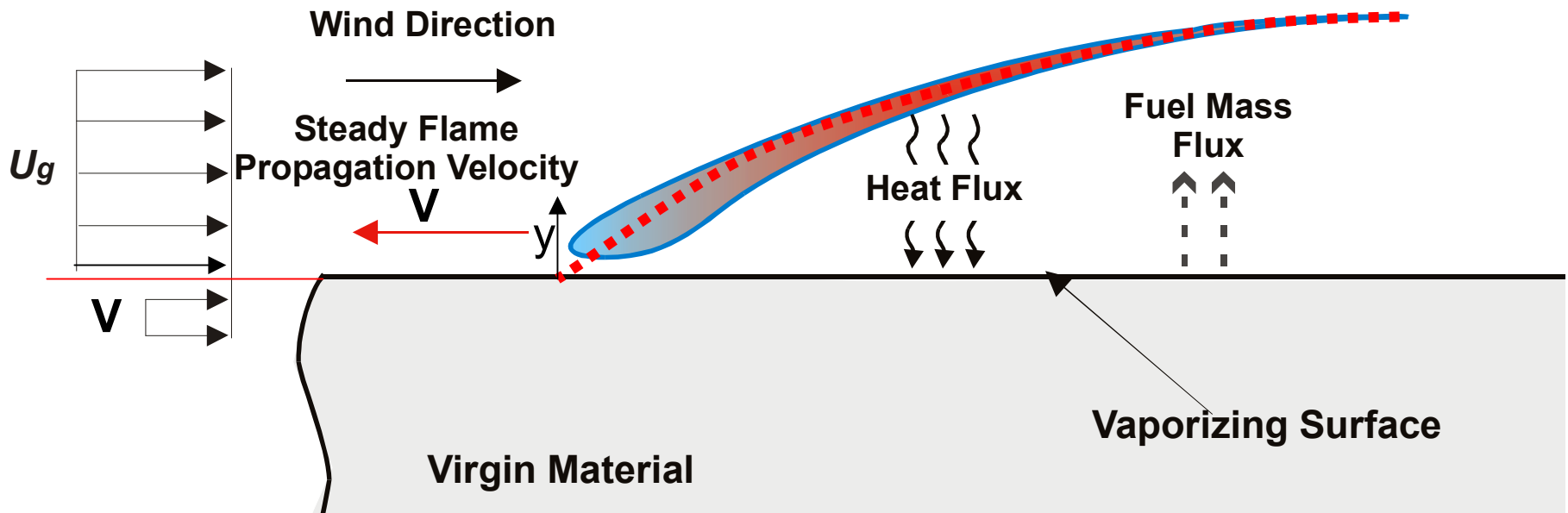
X-axis: TIME (sec)
Y-axis: MASS LOSS ($g/m^2 s$)

In midst of ignorance of appropriate decomposition kinetics, it is O.K to use pyrolysis temperature models.
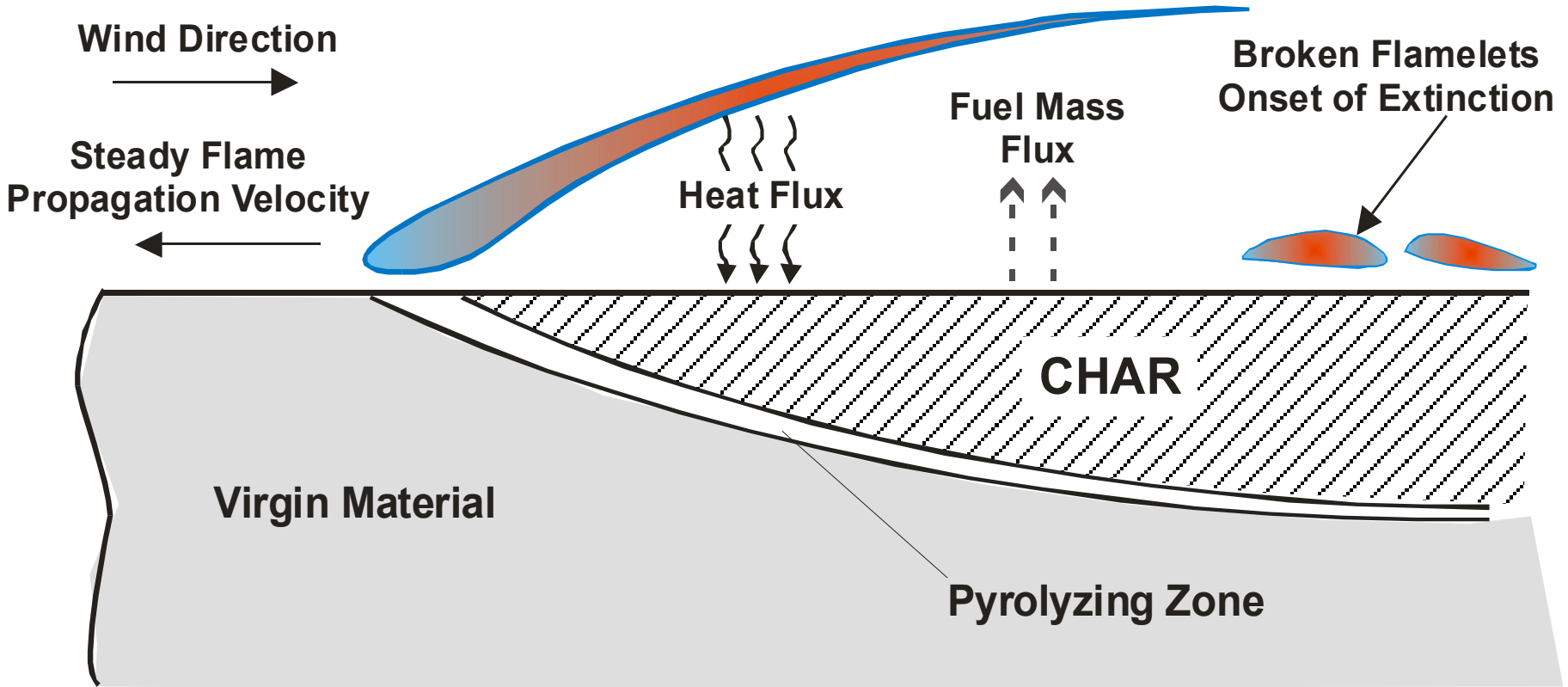
Wind-Opposed Mode of Flame Spread

Numerous experimental & theoretical studies in the last ½ century

deRis, J. N. "Spread of a Laminar Diffusion Flame," <u>Twelfth Symposium (International) on Combustion</u>, P. 241, (1969).
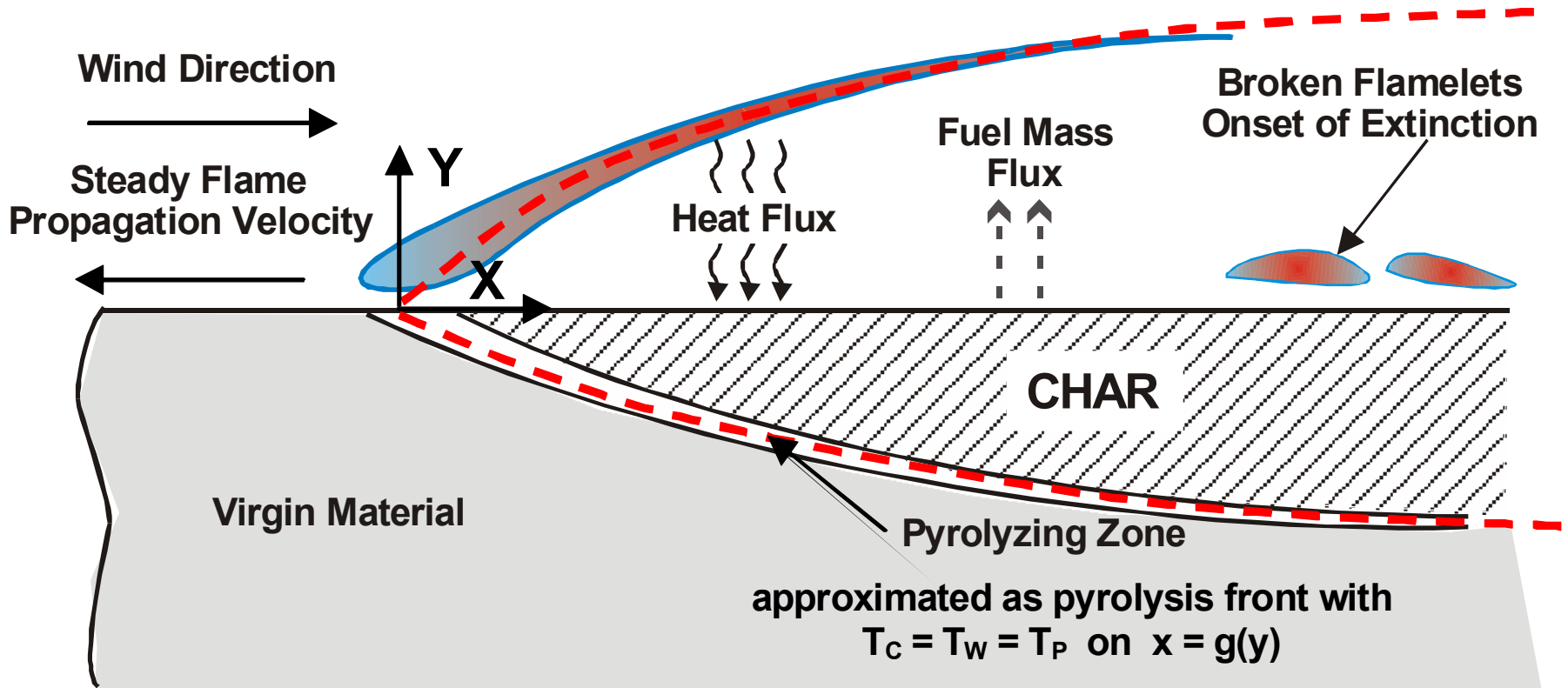

de Ris' formula:
$$V = U_g \frac{\lambda_g \rho_g C_{pg}}{\lambda_w \rho_w C_{pw}} \left[\frac{T_f - T_p}{T_p - T_\infty} \right]^2$$

# Flame Spread over Charring Materials

Wind Direction

Steady Flame Propagation Velocity

Heat Flux

Fuel Mass Flux

Broken Flamelets Onset of Extinction

CHAR

Virgin Material

Pyrolyzing Zone

The Physical Problem

Flame Spread over Charring Materials

Wind Direction

Steady Flame Propagation Velocity

Y

X

Heat Flux

Fuel Mass Flux

Broken Flamelets Onset of Extinction

CHAR

Virgin Material

Pyrolyzing Zone

approximated as pyrolysis front with
$T_C = T_W = T_P$ **on** $x = g(y)$

The Model Problem: The dotted lines show the approximations made in the gas and solid phases. The pyrolysis zone is approximated by a pyrolysis surface and the reaction zone by a flame sheet.

Flame Spread in the Ceiling Configuration
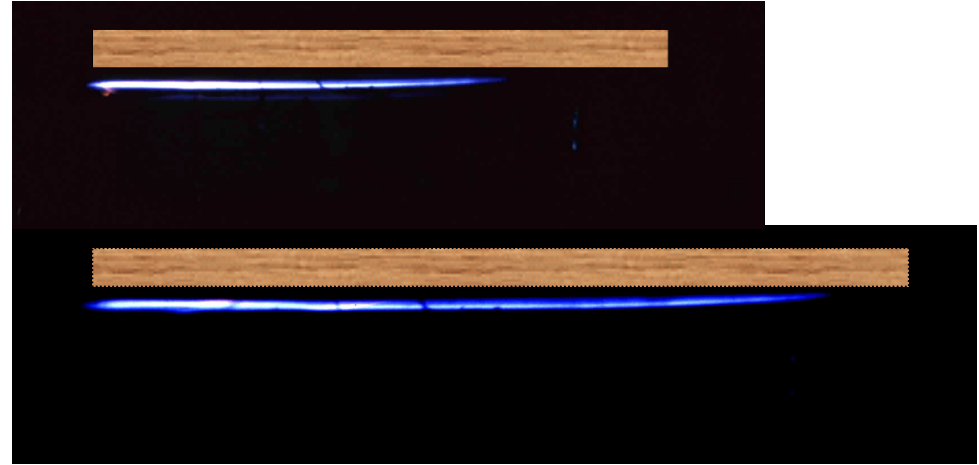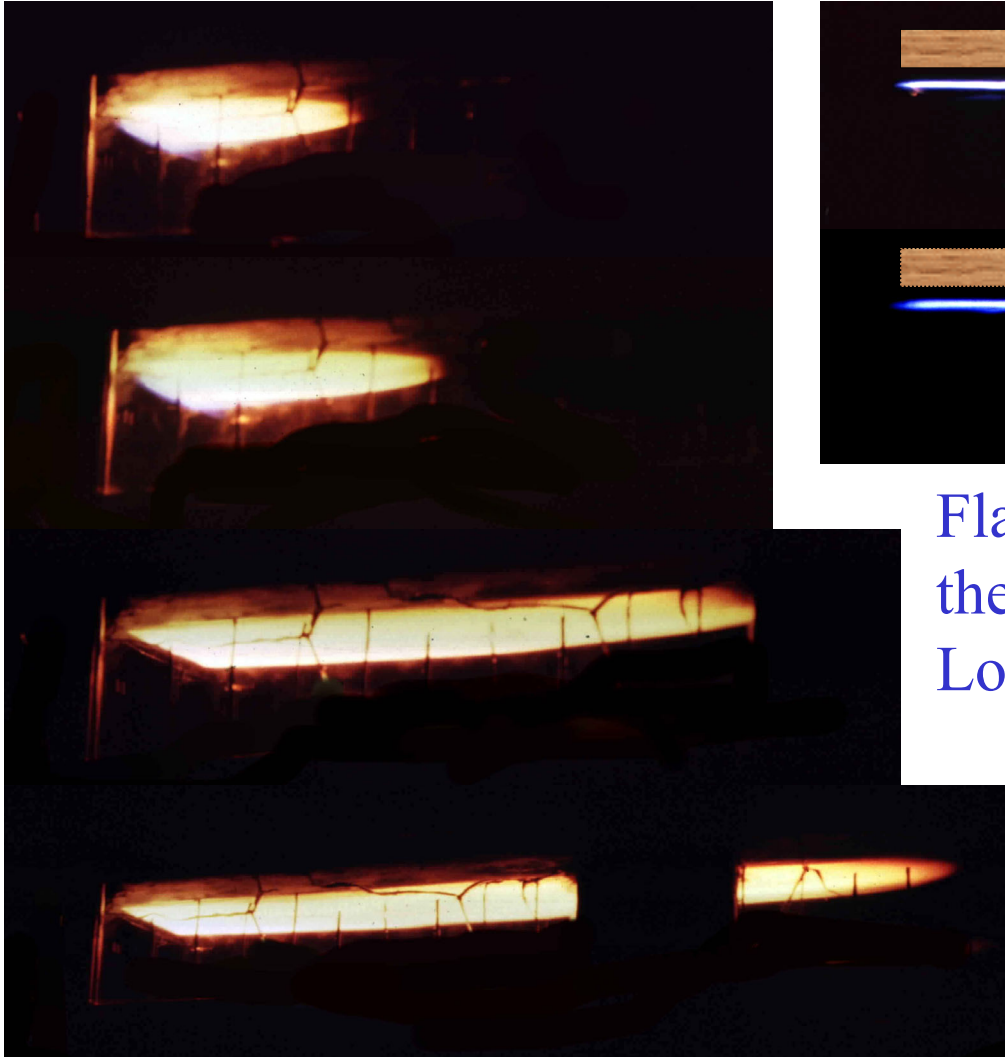
Flame spread on WOOD in the ceiling configuration – Looking edgewise.

Flame spread on PMMA in the ceiling configuration – Looking from below.

MODEL FORMULATION

In the model steady-state coupled elliptic equations for the conservation of mass, energy, species and momentum in the gas-phase and conservation of energy in char and wood are solved exactly using orthogonal parabolic coordinates. The only inexactness is near the leading edge.

The gas-phase equations are transformed by introducing dimensionless parabolic coordinates defined by the expression:

$$\xi + i\eta = \sqrt{\frac{U_\infty}{v_\infty}(x + iy)}$$

While the solid-phase equations are transformed by using:

$$\beta + i\omega = \sqrt{\frac{2V}{\alpha_w}(x + iy)} \; ; \; where \, V \; is \; the \; flame \; speed \; \& \; \alpha_w = {\lambda_w}\big/{\rho_w C_{pw}}$$

Note that, parabolic coordinates impose zero gradient boundary condition on x < 0 & y = 0. However, de Ris'flame spread formula is recovered in the limit of zero char thickness by this analysis.

Flame Spread Solution

The steady flame spread rate is determined by satisfying two physical conditions: These are:

1. The energy balance downstream of the point of flame inception. Along the burning surface ($y = 0; x \geq 0$) it states:

$$-\lambda_g \frac{\partial T_g}{\partial y}(x,0) - \lambda_c \frac{\partial T_c}{\partial y}(x,0).$$

2. This corresponds to the evolution of the fuel mass from the solid & yields the "blowing parameter" m. Note that the pyrolysis products are produced as the char-solid interface (defined by the parabola $\omega = c$) travels through the solid at a constant velocity 'V' converting it to char and generating a mass proportional to ($\rho_w - \rho_c$). This yields the expression for 'm' as:

$$f(0) = -m = -\sqrt{\frac{2\alpha_w V}{v_\infty U_\infty}} \cdot \frac{(\rho_w - \rho_c)}{\rho_{\infty,gas}} \cdot c$$

Flame Spread Solution

The first condition along the burning surface ($y = 0; x \geq 0$) yields:

$$\left(\frac{\mu_0\rho_0}{\mu_\infty\rho_\infty}\right)\left(h_0^s - h_\infty^s - Q_0 Y_{0\infty}\right)\frac{\left[f''(0,m)\right]^{Sc}}{Sc \cdot m \cdot g(\infty, Sc, m)} = \sqrt{\frac{2\lambda_c\rho_c C_{pc}}{\pi\lambda_w\rho_w C_{pw}}}\left(\frac{\rho_w}{\rho_w - \rho_c}\right)\frac{C_{pw}(T_s - T_p)}{c \cdot erf\left(\sqrt{\frac{\delta_c}{2}} \cdot c\right)}$$

Here, $f''(0, m)$ is numerically determined from the Blasius solution for prescribed values of *'m' and Sc*. c – defines the parabolic char-solid interface – it depends entirely on the solid-phase properties. This equation determines an appropriate value of m that satisfies the energy balance at the burning surface. Once *'m'* is determined, the second condition is used to determine the flame spread rate as:

$$\left(\frac{V}{U_\infty}\right) = \left[\left(\frac{c}{m}\right)^2 \cdot \left(\frac{\rho_w - \rho_c}{\rho_{\infty,gas}}\right)^2 \cdot \frac{2\alpha_w}{v_\infty} - 1\right]^{-1}$$

Flame Spread Solution with Oseen Approx.

For the special case of Oseen flow (and imposing de Ris' assumptions the analysis yields the flame spread rate as:

$$\left(\frac{V}{U_\infty}\right) = \frac{\lambda_g \rho_g C_{pg}}{\lambda_c \rho_c C_{pc}} \left[\left(\frac{T_f - T_s}{T_s - T_p}\right) \, erf\left(\sqrt{\frac{\delta_c}{2}} \; c\right)\right]^2$$

In the limit of zero char thickness, i.e. as c $\rightarrow$ 0 (no char) and $T_p \rightarrow T_s$, & we obtain:

$$\underset{\substack{c \rightarrow 0 \\ T_p \rightarrow T_s}}{Lim} \left\{\frac{erf\left(\sqrt{\frac{\delta_c}{2}} \, c\right)}{(T_s - T_p)}\right\} = \sqrt{\frac{\lambda_c \rho_c C_{pc}}{\lambda_w \rho_w C_{pw}}} \left(\frac{1}{T_s - T_\infty}\right).$$

Substitution recovers de Ris' spread formula for 'vaporizing' solids.

The Char-Material Interface

The char-material interface is defined by the parabola $\omega = c$, where the value of 'c' is obtained from the solution of:
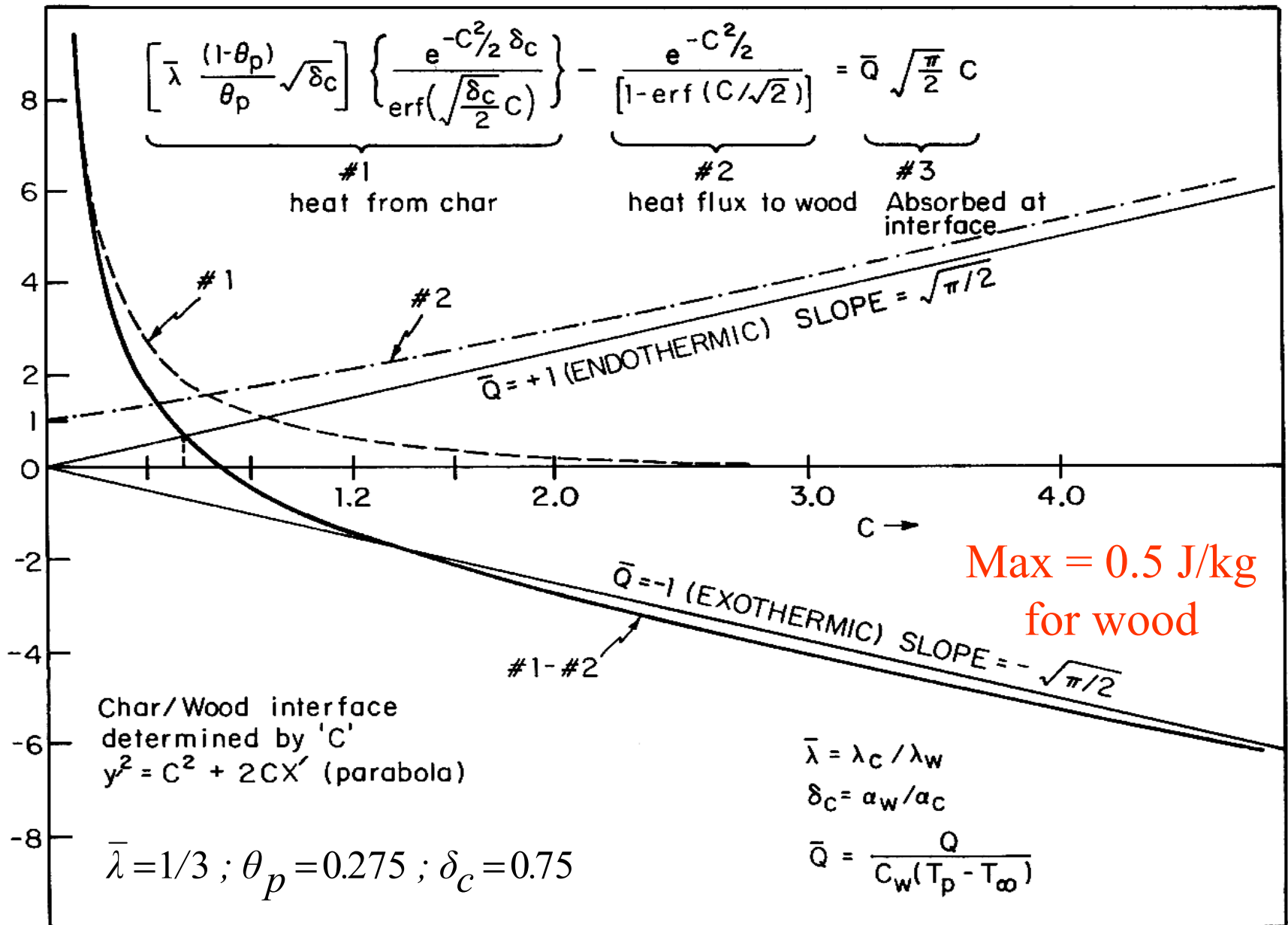
$$\left\{\overline{\lambda}\,\frac{(1-\theta_p)}{\theta_p}\sqrt{\delta_c}\right\}\left\{\frac{\exp\left(-\dfrac{c^2\delta_c}{2}\right)}{erf\left(\sqrt{\dfrac{\delta_c}{2}}\,c\right)}\right\} - \frac{\exp\left(\dfrac{c^2}{2}\right)}{erfc\left(\dfrac{c}{\sqrt{2}}\right)} = \overline{Q}\sqrt{\frac{\pi}{2}}\,c$$

Here, $\delta_c = \left[\left(\dfrac{\lambda_w}{\rho_w C_{pw}}\right)\Big/\left(\dfrac{\lambda_c}{\rho_c C_{pc}}\right)\right]$; $\overline{\lambda} = \dfrac{\lambda_c}{\lambda_w}$ and $\overline{Q} = Q/C_{pw}(T_p - T_\infty)$

$\overline{Q}$ is the Stefan number (+ve for endothermic pyrolysis). Other terms are:

1. the nondimensional heat flux to the interface from char (goes to '0' as $c \to \infty$ and goes to '∞' as c tends to '0')
2. the nondimensional heat flux leaving the interface into the pristine solid (goes to '1' as c goes to '0' and goes to '∞' like c as c tends to '∞'
3. the heat absorbed or liberated at the char-solid interface. The solution requires four input parameters: $\overline{\lambda}, \overline{Q}$, δ_c and θ_p.

Determination of the Char-Material Interface

$$\left[\bar{\lambda}\,\frac{(1-\theta_p)}{\theta_p}\sqrt{\delta_c}\right]\left\{\frac{e^{-C^2/2\,\delta_c}}{erf\left(\sqrt{\frac{\delta_c}{2}}\,C\right)}\right\} - \frac{e^{-C^2/2}}{\left[1-erf\left(C/\sqrt{2}\right)\right]} = \bar{Q}\sqrt{\frac{\pi}{2}}\,C$$

#1 heat from char   #2 heat flux to wood   #3 Absorbed at interface

$\bar{Q}=+1$ (ENDOTHERMIC) SLOPE = $\sqrt{\pi/2}$

$\bar{Q}=-1$ (EXOTHERMIC) SLOPE = $-\sqrt{\pi/2}$

#1 - #2

Max = 0.5 J/kg for wood

Char/Wood interface determined by 'C'
$y^2 = C^2 + 2CX'$ (parabola)

$\bar{\lambda} = \lambda_c/\lambda_w$
$\delta_c = \alpha_w/\alpha_c$
$\bar{Q} = \dfrac{Q}{C_w(T_p - T_\infty)}$

$\bar{\lambda}=1/3$; $\theta_p=0.275$; $\delta_c=0.75$

Isotherms inside the semi-infinite charring solid

representative values for wood : $\bar{\lambda}=1/3$; $\theta_p=0.275$; $\delta_c=0.75$
$\bar{Q}=1.0$; $c=0.53$

$\theta_c=1,\ T=T_s$

$\theta_c=0.675$

CHAR

$\theta_c=0.475$

$\bar{Q}=1.0$

CHAR $\theta=\theta_p=0.275$

WOOD

VIRGIN MATERIAL

$\theta_w=0.175$
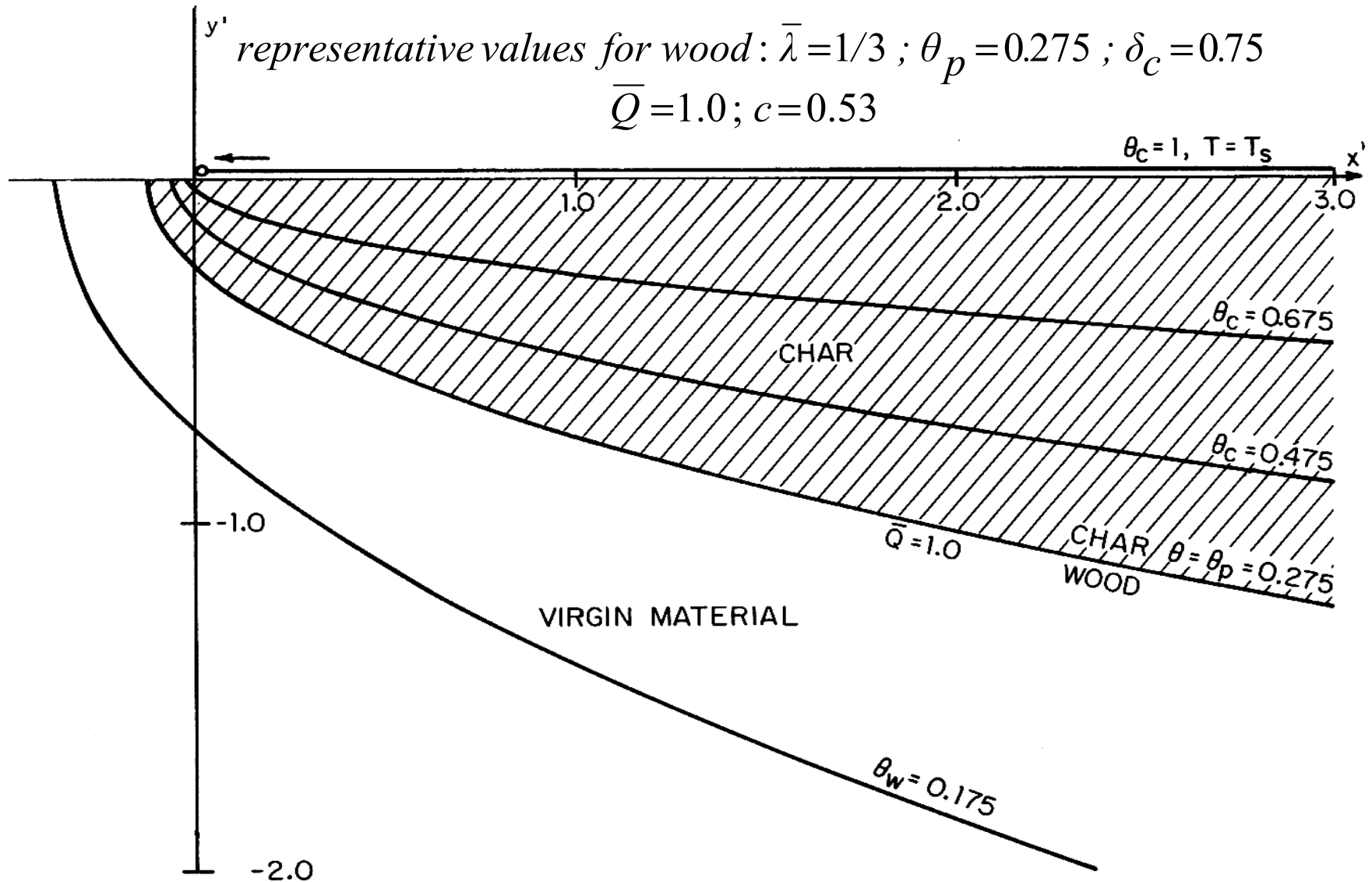
The Flame Spread Rate

Velocity and mixture fraction profiles inside the boundary layer

Sc = 0.7 for all calculations

y-axis: $\zeta = \dfrac{1}{2}\sqrt{\dfrac{U_\infty}{\nu_\infty x}}\displaystyle\int_0^y \dfrac{\rho(Z)}{\rho_\infty}\, dy \rightarrow$

x-axis: $Velocity \rightarrow f'(0) = 2u/U_\infty,\ \&\ Mix.Fract. \rightarrow Z(\zeta)$
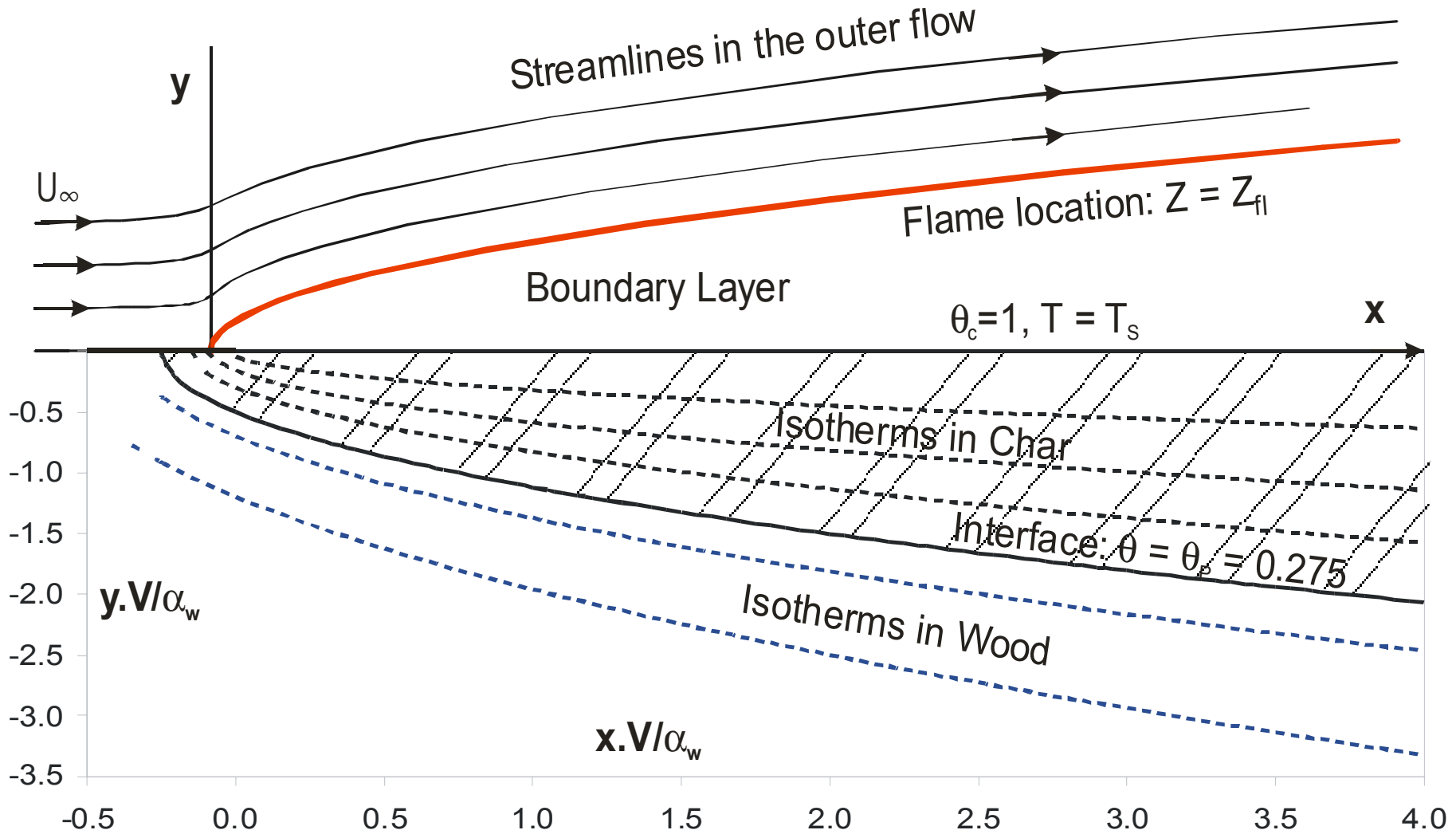
Curve labels: $m=1.2$, $m=1.0$, $m=0.0$
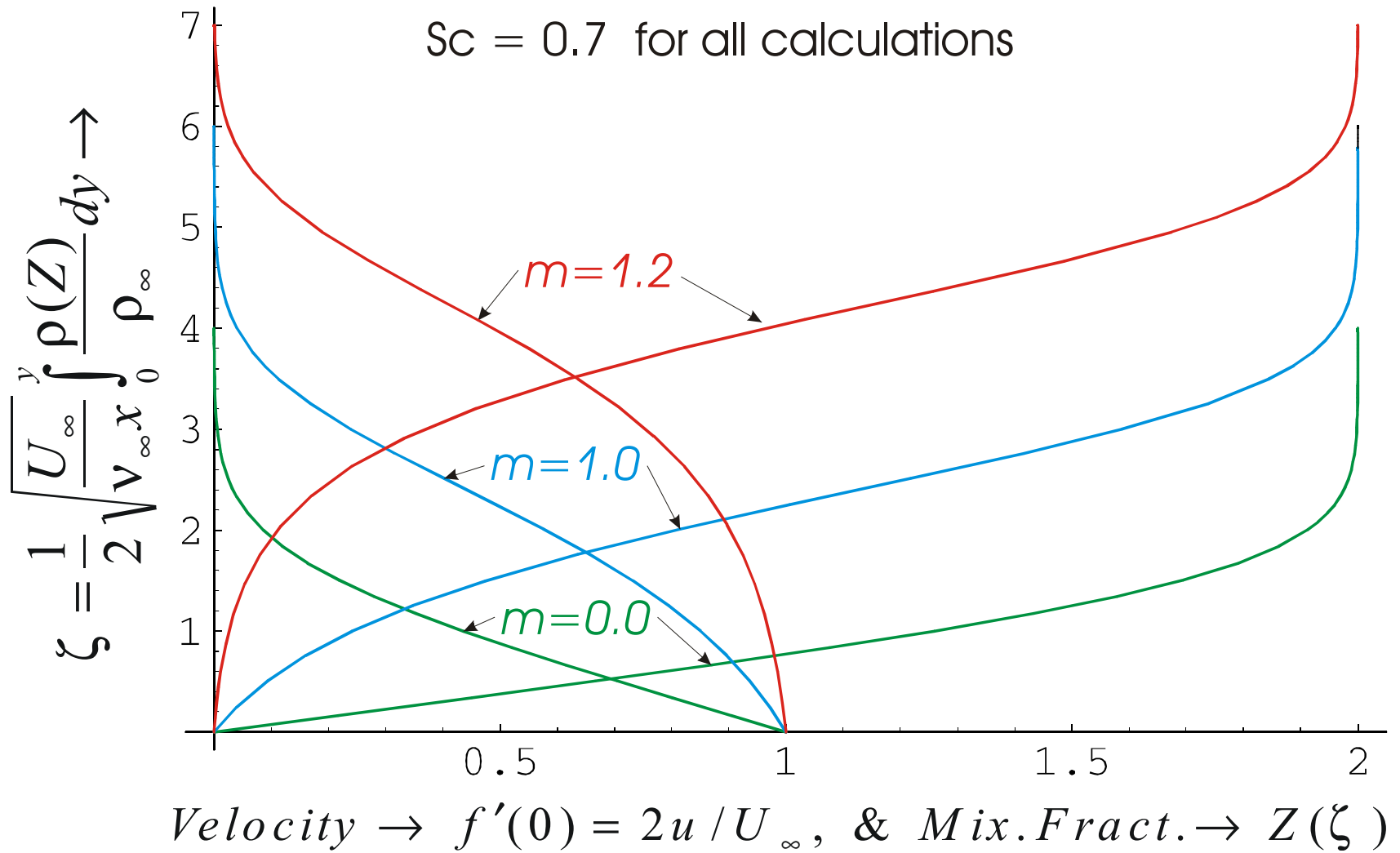
The Flame Spread Rate

Variation of the flame spread velocity normalized by the free-stream velocity for various values of 'm' and 'c'
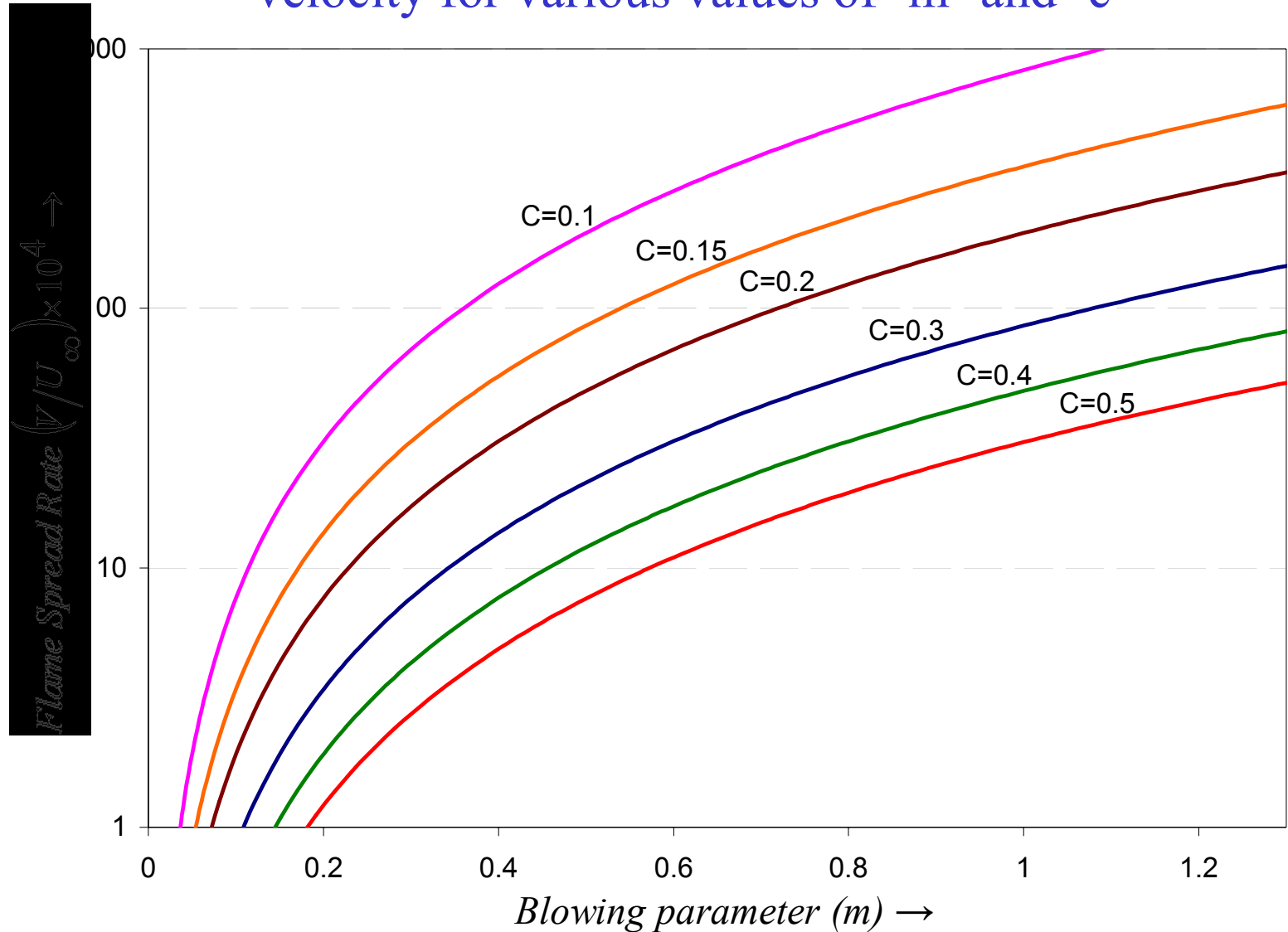
The Flame Spread Rate

Calculated stream lines and the flame location in the gas-phase along with the calculated isotherms in wood and char shown for c = 0.501.
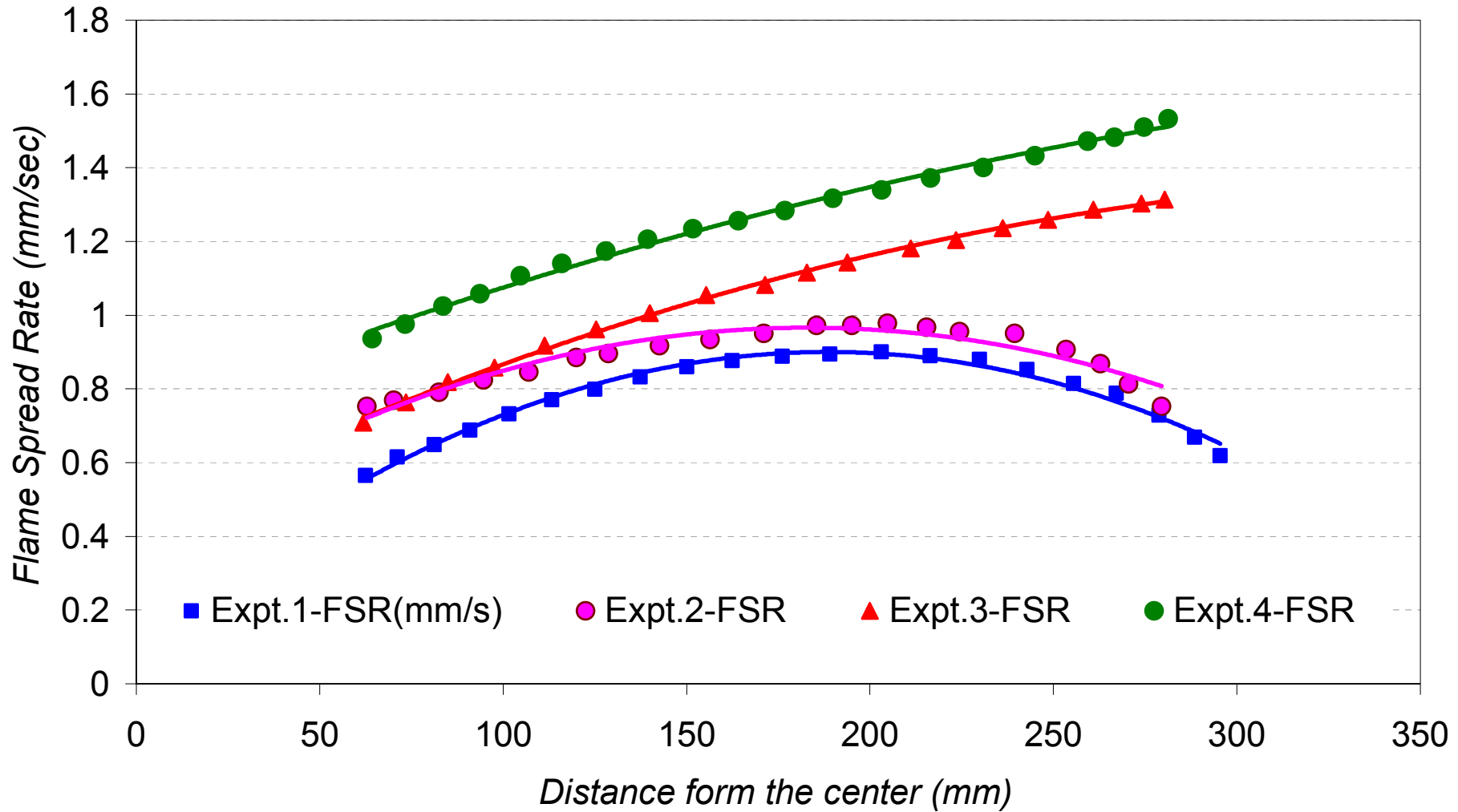

U_∞

Streamlines in the outer flow

Flame location: $Z = Z_{fl}$

Boundary Layer

$\theta_c = 1$, $T = T_s$

x

Isotherms in Char

Interface: $\theta = \theta_p = 0.275$

$\mathbf{y.V}/\alpha_w$

Isotherms in Wood

$\mathbf{x.V}/\alpha_w$

Flame Spread Experiments on Wood in the Horizontal Configuration

Horizontal Configuration
MEASURED FLAME SPREAD RATE

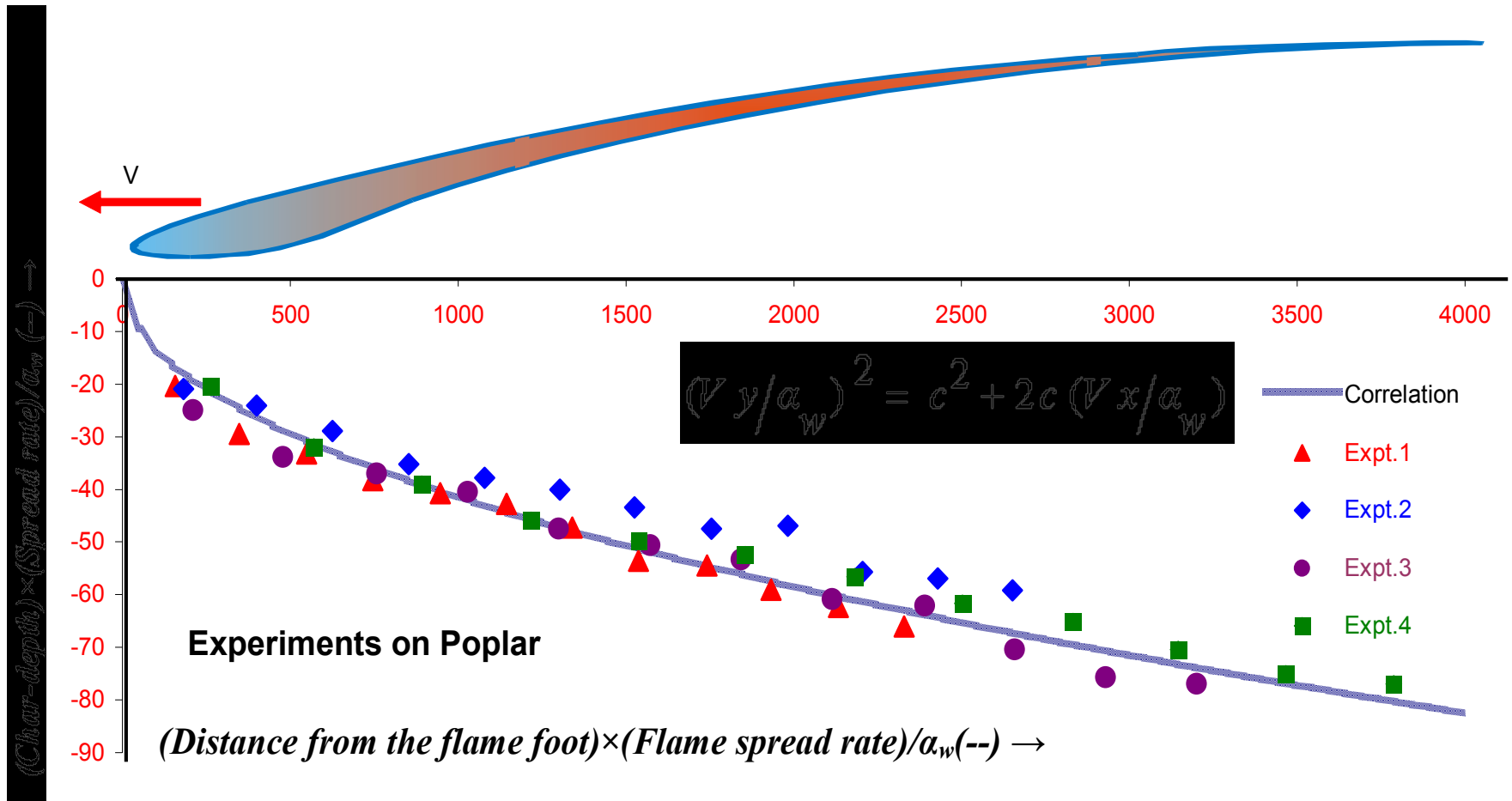Legend: Expt.1-FSR(mm/s) ● Expt.2-FSR ▲ Expt.3-FSR ● Expt.4-FSR

Y-axis: Flame Spread Rate (mm/sec)

X-axis: Distance form the center (mm)

Horizontal Configuration
MEASURED CHAR DEPTH

Distance from the flame foot (mm)

Char depth (mm)

Expt.4-CD   Expt.2-CD   Expt.3-CD   Expt.1-CD
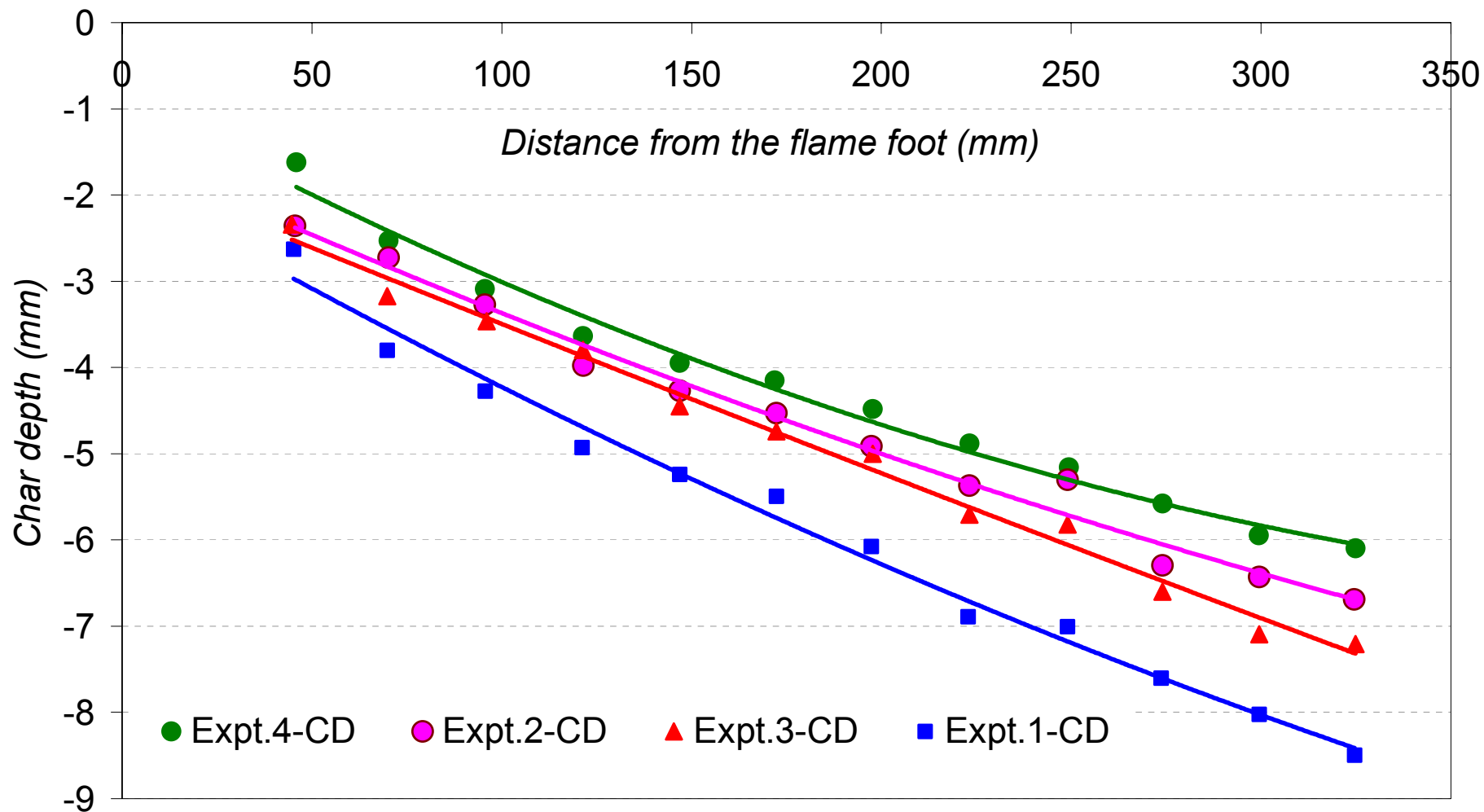
The Flame Spread Rate

Measured flame spread rates and char depths are correlated. Clearly, smaller char-depths are produced by higher flame speeds.

$$\left(V\,y/\alpha_w\right)^2 = c^2 + 2c\left(V\,x/\alpha_w\right)$$

Correlation

▲ Expt.1

◆ Expt.2

● Expt.3

■ Expt.4

Experiments on Poplar

(Distance from the flame foot)×(Flame spread rate)/α_w(--) →

((Char-depth)×(Spread rate)/α_w (--)) →

Conclusions

1. This analysis develops a theoretical description of a diffusion flame spreading against the wind on a semi-infinite charring solid.

2. Using the pyrolysis temperature and flame sheet approximations, the steady-state coupled elliptic equations for conservation of energy, mixture fraction and momentum in the gas-phase and conservation of energy in char and wood are solved exactly.

3. A more general analytical solution is presented that reduces to de Ris' flame spread formula in the limit of zero char thickness and with similar assumptions.

4. The growing char layer in the solid-phase has considerable influence on the flame spread rate. It is seen that formation of a thicker char layer significantly retards the spread rate.

Conclusions (contd.)

4. Unique steady-state solutions for the parabolic char-material interface were found to exist only for Stefan number > -1. For Stefan number = -1 (i.e., exothermic), two solutions were found. One of these solutions corresponds to the location of the char-solid interface at infinity, indicating the likelihood of a thermal runaway. This happens regardless of the property values.

5. Measured char thickness, even for experiments on flame spread over (rather than under) horizontal surfaces of wood, correlate well according to this formula. As expected, faster flame spread produces thinner char.

6. The location of the parabolic char-material interface depends upon:

    a) The ratio of thermal conductivities and thermal diffusivities of the char and pristine solid.

    b) The nondimensional pyrolysis temperature, and

    c) The Stefan number.

Conclusions (contd.)

7. Calculations using the available property data for wood and its char provide much insight into the controversial heat of thermal decomposition of wood. It is found that a value greater than 0.5 J/Kg of wood (exothermic) will result in a thermal runaway – a phenomenon that has not been observed. This raises serious doubts about the reported exothermic heats of thermal decomposition of wood, some of which are more than three times greater than the theoretical limiting value.